The coupling effects of thermal cycling and high current density on Sn58Bi solder joints

Yong Zuo · Limin Ma · Sihan Liu ·
Ting Wang · Fu Guo · Xitao Wang

Abstract Currently, one of the serious challenges in microelectronic devices is the miniaturization trend of packaging. As the decrease of joint dimension, electromigration (EM) and thermomechanical fatigue become critical issues for fine pitch packaging. The independent mechanisms of EM and thermomechanical fatigue are widely investigated and understood. However, the coupling effect of both conditions needs further exploration. The current study established the correlation between resistance and microstructure evolution of solder joint under the combination effect of thermal cycling and high current density and illustrated the different contributions of these two factors to the reliability of the joint through the comparison monopoly tests. The results revealed that cracks had more impact on resistance increase than phase segregation. The resistance evolution could be divided into three stages. First, the resistance mitigated due to the phase coarsening. Second, Joule heating effect made the resistance increase slowly. Third, EM led to the resistance increase rapidly. The high current density can help to improve the reliability of the solder joint under the coupling effect of thermal cycling and EM at the initial stage, but harmful to the consequence process.

Y. Zuo · L. Ma (✉) · S. Liu · T. Wang · F. Guo
The College of Materials Science and Engineering,
Beijing University of Technology, Beijing 100124,
People's Republic of China
e-mail: malimin@bjut.edu.cn

F. Guo
e-mail: guofu@bjut.edu.cn

X. Wang
State Key Laboratory for Advanced Metals and Materials,
University of Science and Technology Beijing, Beijing 100083,
People's Republic of China

Introduction

Owing to the higher requirements for multifunctional of portable devices, one of the main challenges faced by the microelectronic packaging is the miniaturization trend of solder bumps which usually play an important role on both the mechanical support and electrical connection for the circuit board. On one hand, the size reduction of solder joint means the threat from thermal cycling becomes more severe due to the coefficient of thermal expansion (CTE) mismatch between the various materials in the packaging during the alternating load like thermal cycling [1, 2]. The thermomechanical fatigue (TMF) process begins with the accumulation of damage at a local region and eventually leads to the formation of cracks and its subsequent propagation [3]. Generally, the cracks originate more easily at the brittle-hard phase which causes significant stress concentration such as IMC layer, Cu_6Sn_5 [4–6]. The growth of cracks reduces the remaining cross-sectional area which in turn increases the current density if imposition of current density on the solder joint. On the other hand, the size continuing scaling down causes current density dramatically increase which will be high enough to drive the mass movement along the electron flow, that is, electromigration (EM) [7]. Since the movement of metal atoms/ions from cathode to anode can be observed in solder during EM to form valley and hillock, respectively [8, 9]. For two-phase solder materials such as Sn–Pb, Sn–Bi, etc., phase segregation could occur due to the divergence of the diffusion rates between two elements [9–13]. EM also accelerates the growth rate of intermetallic compound (IMC) layer at the anode and leaves vacancies at the cathode which companies by the phase coarsening [8, 11, 14]. The voids are harmful to the joint under TMF condition and contribute to the degeneration of mechanical performance of solder joint.

The failure mechanisms of EM and TMF induced by electrical load and thermal cycling are widely investigated and understood, respectively. However, the combination effect of these two factors has earned rare attention. Some of the studies have discussed the stress and microstructure changes in grain size scale under such condition through synchrotron X-ray technology, but none of them in macroscopic scale [9, 15]. The previous literatures also show that both cracks and phase segregation give rise to the resistance change of solder joint [16–18]. Therefore, it is necessary to study the solder joint which suffered the coupling interactions of electric current and thermal cycling and illustrate the combination failure mechanisms through the comparison tests with individual effects on solder joint. Besides, the development of future solders should focus more on the alloys which with low melting temperature and cost effectiveness when considered that the current Pb-free solders reflowed at a higher temperature and more expensiveness than conventional eutectic Sn–Pb alloy. Thereafter, as one of premising candidates, eutectic Sn–Bi solder has earned many attentions [19].

The purpose of this investigation is to understand the combination effects of current density and thermal cycling on resistance evolution of the joint and further reveal the relationship between the microstructure and resistance. A one-dimensional Cu/Sn58Bi/Cu linear solder joint was applied to ensure the uniform distribution of current density through the whole joint. The resistance and microstructure characterizations were simultaneously collected and observed during the test period, respectively. Moreover, the relationship between microstructural evolution and ambient conditions was established.

Experimental procedures

The eutectic Sn58Bi solder ball with a diameter of 500 μm was provided by Accurus Scientific Co., Ltd. The solder ball was pressed into a 200-μm thick solder sheet by spiral micrometer. Then the solder sheet was applied to fabricate the joint so as to ensure the thickness of joint. A specially designed aluminum die was used to help the fix of the Cu/solder/Cu solder joint structure. Two copper substrates were cross headed with a solder sheet between them and banded in a reflow oven system as shown in Fig. 1a. The solder joint was mounted with epoxy resin (Fig. 1b) for the subsequent treatment. Then the sample was ground to a triangular prism structure. When the width of hypotenuse of the triangular prism was 447 μm, the area of cross section of solder joint was 5×10^{-4} cm^2 as shown in Fig. 1c, d. Then a 5 A direct current could produce an average current density of 10^4 A/cm^2 throughout the solder joint which was considered to be the threshold for EM [20]. More details of solder joint preparation could be found in previous publication [12].

Four probes method which could avoid the contact resistance was applied to collect the resistance data of solder joint during the variation experiments as shown in Fig. 2. Two voltmeter probes were connected inside the two DC probes. Thermal cycling environment provided by Sida® Temperature Impact Test Chamber. Figure 3 described the temperature curve of the thermal couples which attached on the joint during the thermal cycling test. A sound cycle would take 5 h. Both of the dwell times at high and low extreme temperatures were 2 h and the heating and cooling rates were 3 and 2 K/s, respectively. Paperless recorder MV2000® which could acquire ten

Fig. 1 Structure and dimensions of solder joint. **a** Fixture, **b** the mounted solder joints, **c** as fabricated of the specimen, **d** dimensions and structure of joint
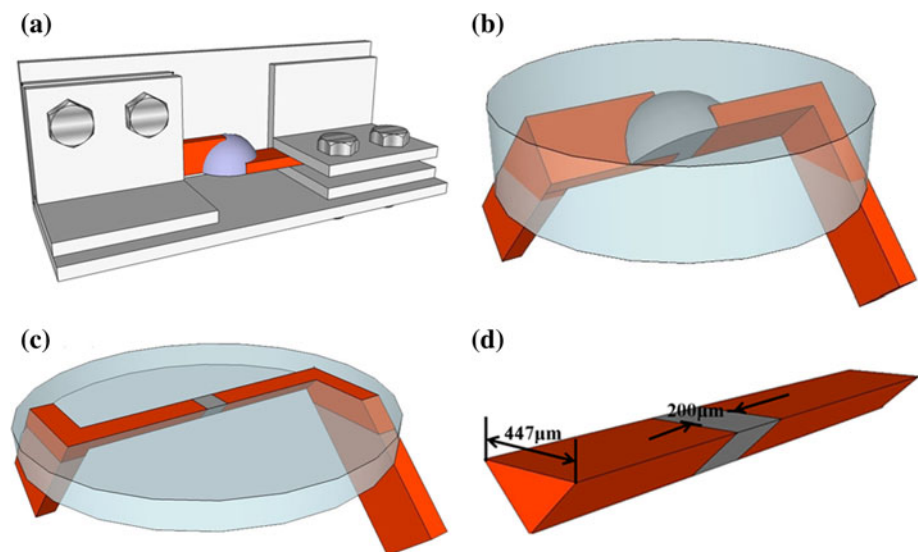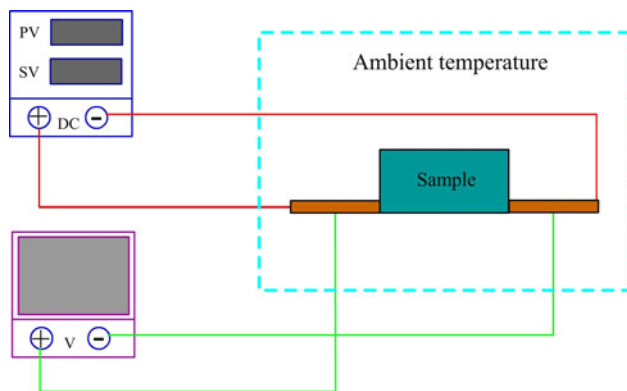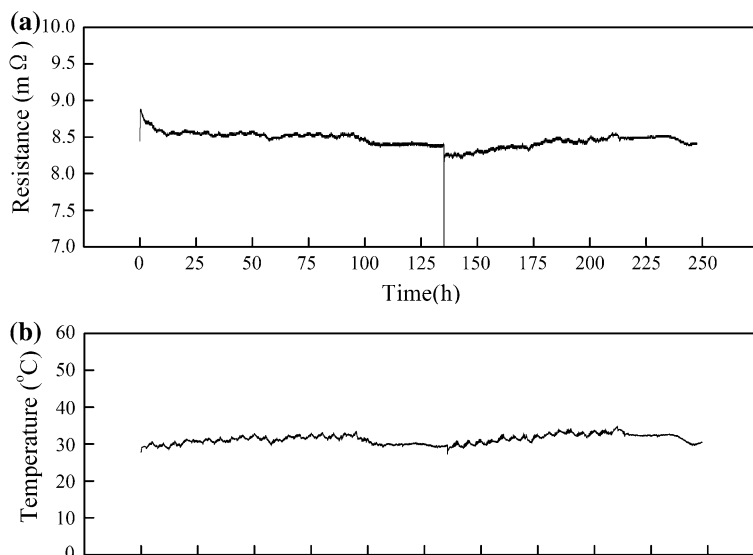
Fig. 2 The schematics of voltage acquisition setup
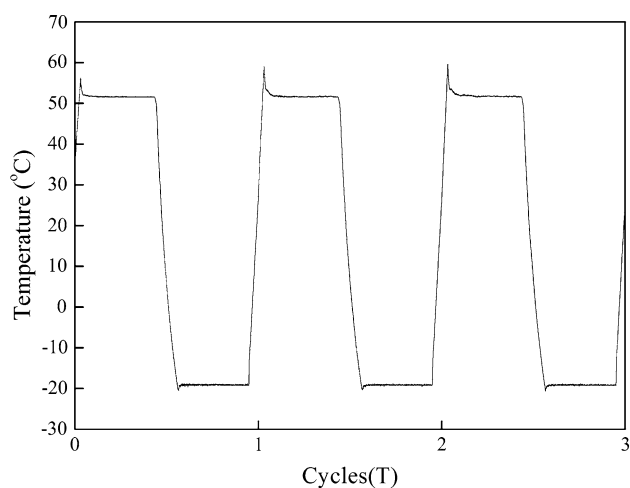
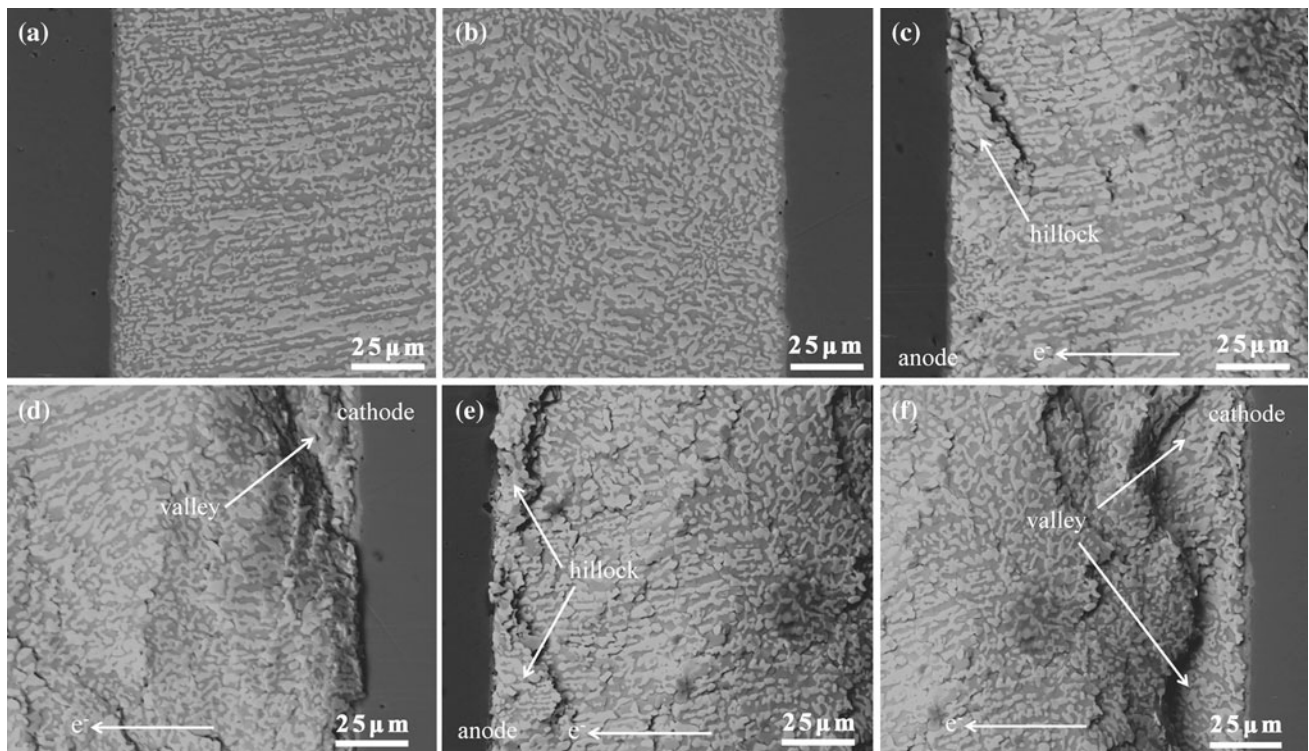Fig. 3 Temperature profile of the solder joints under the thermal cycling condition

channels data simultaneously was implemented to collect voltage and temperature data. Details of schematic of the experimental setup were shown in Fig. 2. Origin® software and scanning electron microscope (SEM) were used to analyze the resistance data and microstructure observation, respectively.

Results

Current stressing at room temperature

In order to illustrate the individual roles on reliability issues of solder joint, a series of comparable experiments were carried out in current study. Figure 4a shows the resistance change of the solder joint under the current stressing of 10^4 A/cm^2 at room temperature for 250 h. The temperature profile of the joint was given by Fig. 4b through an attached thermal couple to interpret the fluctuations of the resistance which induced by temperature due to the resistivity as a function of temperature. It was believed that the evolution of resistance was almost consistent with temperature change except for the initial 50 h. Resistance decreased at the beginning of current stressing. This phenomenon could be explained by the corresponding microstructure characterizations as shown in Fig. 5.

After current stressing for 135 h, the hillock and valley could be observed compared with Fig. 5a–d, respectively. Besides, phase coarsening is also evident in solder matrix. The resistance decreased at the initial stage of current stressing due to the phase coarsening which reduced the total internal phase boundary as shown in Fig. 4. The number of free electrons which scattered by the phase boundary were diminished and caused the resistance

Fig. 4 The evolution of **a** resistance value and **b** temperature of the solder joint under the current stressing 10^4 A/cm^2 at room temperature for 250 h

Fig. 5 Microstructure characterizations of SnBi solder joint under current stressing of 10^4 A/cm^2 at room temperature (**a**, **b**) as reflowed, anode (**c**) and cathode (**d**) EM for 135 h, anode (**e**) and cathode (**f**) EM for 250 h

decrease. During this period, mass transportation was not severe because of the high activation energy of EM at room temperature [11].The typical EM characteristics of eutectic SnBi solder was plastic deformation and phase segregation which produced continuous Bi-rich phase and Sn-rich phase at anode and cathode, respectively [13, 14]. No obvious phase segregation could be found even after current stressing for 250 h as shown in Fig. 5e, f. Thereafter, the effect of plastic deformation would play a more important role than phase segregation and grain coarsening on resistance change during the consequence of EM and led to rise of the resistance with the increase of current stressing time. Further deformation caused by hillock and valley contributed to the increase of the resistance due to the decrease of contact area between solder and substrate.

Thermal cycling with low current density stressing

There were two factors influencing the resistance variation. One is temperature fluctuation during thermal cycling process. The other one is the microstructure evolution such as the formation of voids and the propagation of cracks. These microstructure changes reduced the contact area between solder and substrate and changed the resistance value. Voltage acquisition method was based on the promise of electric current applying to the conductor. In order to avoid the EM effects, a low current stress with the current density
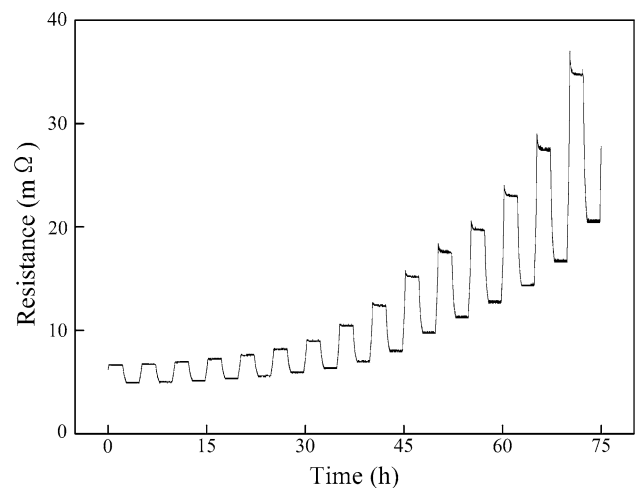
Fig. 6 The resistance evolution of the solder joint under the thermal cycling ranged from −20 to 50 °C for 15 cycles

of 2×10^2 A/cm^2 was introduced in this experiment which had no EM impact on microstructure evolution and ensured that the resistance could be monitored as well. Figure 6 shows the resistance evolution with the thermal cycling time. The sample experienced the thermal cycling ranged from −20 to 50 °C for 15 cycles. The resistance values of peak and valley exponentially increased with time. Resistance raised from 6 mΩ to over 30 mΩ only took 75 h. It demonstrated that the microstructure of solder joint suffered

serious degeneration process during thermal cycling. The reduction of cross-sectional area of solder joint led to the increase of the resistance.

The corresponding microstructure was examined after thermal cycling 75 h as shown in Fig. 7c, d. Compared with as reflowed condition (Fig. 7a, b), drastically deterioration of microstructure could be observed. Cracks formed and propagated along both sides of Cu/solder interfaces. Moreover, Bi colony and Sn-rich phase disintegrated individually along their phase boundaries in some regions. These cracks and fractured boundaries reduced the cross-sectional area of solder joint and boosted the raise of resistance. IMC layer more easily suffered stress concentration and at which damages accumulated and caused crack initiation and subsequently propagation due to the CTE mismatch between solder and substrate materials during the thermal cycling [2]. It should be noted that SnBi itself also had CTE mismatch problem due to its lamellar microstructure characterization. The whisker can be examined from Fig. 7e which was the evidence that the stress concentration accumulated between Sn-rich and Bi-rich phases and became the squeeze sites for whisker. Besides, no phase segregation could be observed from Fig. 7. The mass transportation had no influence on the above results. Thereafter, the effect of low electric current density on solder joint can be ignored when mentioned to acquisition the voltage data. The resistance profile of Fig. 6 could be comprehended as only impacted by thermal cycling.

Thermal cycling with high current density stressing

Figure 8 plots the resistance evolution with the coupling effect of current stressing of 10^4 A/cm^2 and thermal
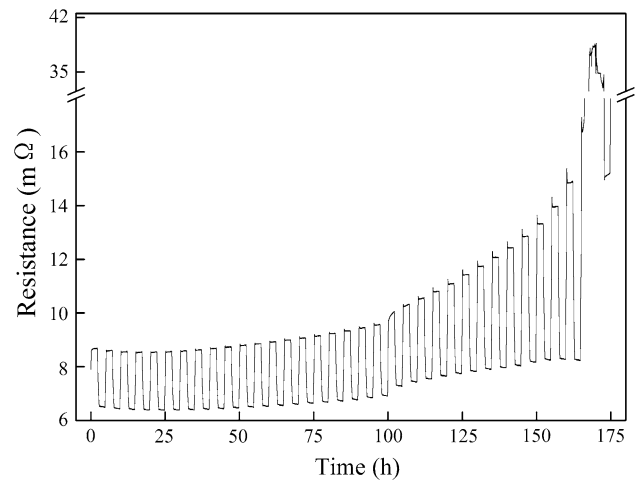
Fig. 8 The resistance evolution of the solder joint under the coupling effect of thermal cycling ranged from −20 to 50 °C and high current stressing of 10^4 A/cm^2 for 35 cycles
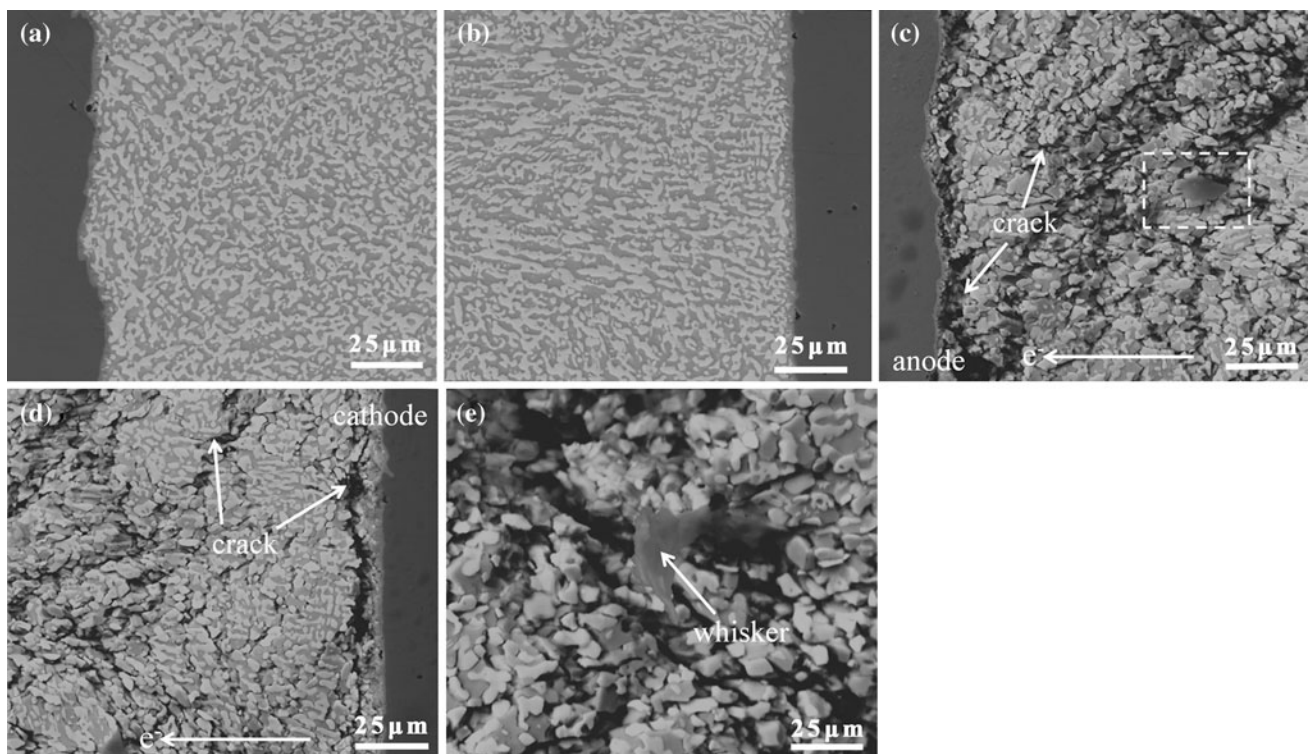
Fig. 7 Microstructure characterizations of SnBi solder joint under thermal cycling ranged from −20 to 50 °C. (a, b) as reflowed, anode (c) and cathode (d) after 15 cycles, (e) enlarged image of the *dashed box* in (c)

cycling ranged from −20 to 50 °C for 175 h. In the early 30 h, the resistance values of peak and valley both decreased slightly. Subsequently both of them rose slowly till 100 h. Then the increase rate of resistance speeded up at high temperature dwell period while slowed down at the low temperature dwell time. Finally a resistance jump could be observed from the last cycle which indicated the failure of the solder joint at the high temperature stage. It was worth noting that the growth rate of resistance and lifetime of the joint which suffered the combination effect of thermal cycling and high current density was much slower and longer than that of the joint only experienced the thermal cycling (or the coupling effect of thermal cycling and low current density) when compared Fig. 8 with Fig. 6. Moreover, phase segregation emerged in Fig. 9. The high current density improved the lifetime of the solder joint.

Figure 9 provides the SEM images of solder joint after different thermal cycles with high current density stressing. Typical SnBi lamellar microstructure could be seen as reflowed condition (Fig. 9a, b). Cracks formed inside the solder matrix after 20 cycles and it was clear that the cracks propagated along the phase boundary between Bi-rich phase and Sn-rich phase and no crack could be detected at the interface areas as illustrated in Fig. 9c, d. After 35 cycles, a continuous Bi-rich phase layer observed at anode interface obviously and the solder deformed seriously as seen in Fig. 9e, f. Besides, a thicker IMC layer also formed at the cathode side when examined the polished surface of the joint as shown in Fig. 9g, h. At the cathode, some of the larger Cu_6Sn_5 colonies located close to IMC layer and the

morphology of interface was convex to the substrate side. EM effect made the copper atoms dissolved into solder along the direction of electron flow and led to the formation of Cn_6Sn_5 IMC in solder matrix and wave type IMC layer at the initial stage of EM [8]. At the anode, a continuous Bi-rich layer with a contiguous Sn-rich layer formed close to interface. These results suggested that EM damages far more severely at the high current density stressing than low density. It should be pointed out that the cracks formed between Bi-rich layer and Sn-rich layer at the anode, but not at the IMC layer as reported by several literatures [4–6]. This result might demonstrate that the bond strength of Bi/Sn was lower than the Cu_6Sn_5/Bi.

Discussion

It was interesting to note that the mean time to failure of the joint under the coupling effect of thermal cycling and EM was even longer than that of the joint just suffered the thermal cycling. This might be due to the enhanced performance of the solder joint by Joule heating effect at low temperature. It not only retarded the formation of crack at low temperature, but also inhibited the rapid raising of the resistance at the initial stage as well. It was well known that solder joint became more brittle at low temperature extreme stage. Besides, the thermal shock from the temperature ramp (CTE mismatch) and stress concentration made the nucleation of crack more severe at low extreme stage than high temperature dwell time and its further propagation was very rapid once the cracks initiated when
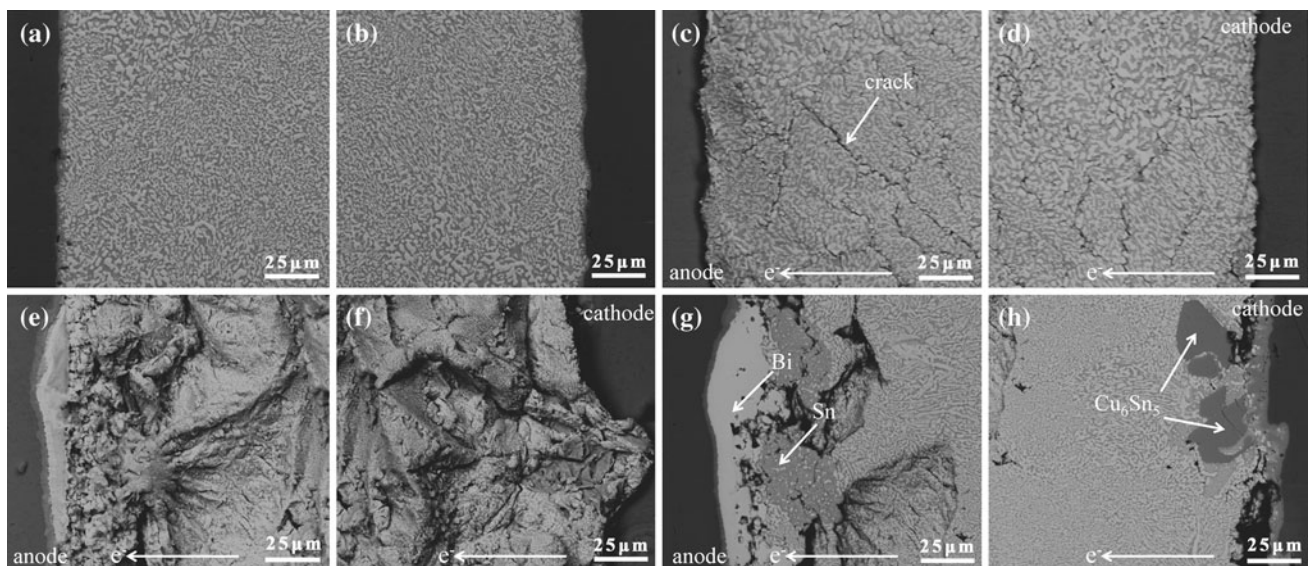
Fig. 9 Microstructure characterizations of the SnBi solder joint under the coupling effect of thermal cycling ranged from −20 to 50 °C and current stressing of 10^4 A/cm^2 for 35 cycles (a, b) as reflowed, anode (c) and cathode (d) after 20 cycles, anode (e) and cathode (f) after 35 cycles (g, h) are the microstructure of (e) and (f) after polished

considered that the stress relaxation and the compliant of alloy declined with the temperature decrease [2]. Thereafter, the reliability of solder joint can be reinforced by improving the low extreme temperature and the range between high and low temperature of the thermal cycling. The high current density applied in this test caused an obvious Joule heating effect. It was indicated that the actual temperature of low extreme temperature was higher than −20 °C. Thus, the high current density alleviated the damage from thermal cycling at the initial stage.

Besides, the resistance change rates of the joint under thermal cycling condition was faster than that of the joint under coupling effect as shown in Figs. 6 and 8. Under the mono thermal cycling condition, the resistance of the joint exceeded 15 mΩ after 10 cycles. However, the resistance of the joint under coupling effect still kept under 15 mΩ before the failure (34 cycles). It was believed that cracks and phase segregation contributed the increase of resistance. Thermal cycling and EM resulted in the formation of cracks and phase segregation, respectively, as shown in Figs. 7c and 9g. Thereafter, the effect of cracks which nucleate and propagate at low extreme temperature during thermal cycling process on the raise of resistance is far more effective than the phase segregation which results from EM.

However, the resistance increased sharply before the final failure should also be noted as shown in Fig. 8. Actually, the main effects of EM on eutectic SnBi solder were Joule heating effect, phase segregation, and mass transportation. Joule heating effect could improve the reliability of the solder joint which suffered the thermal cycling simultaneous and retarded the increase of resistance. Phase segregation had little impact on resistance raise as mentioned above. However, mass transportation could leave vacancies at cathode and accelerate the nucleation of crack at this side. After the initial stage of coupling effect, EM enhanced the propagation of the crack at cathode and became harmful to the thermal cycling.

Figure 10 shows the reduction of relative cross-sectional area with cycle numbers under the coupling effect of thermal cycling and EM. It could reflect the resistance evolution when considered that the resistance is directly proportional to the reduction of relative cross-sectional area. The resistance evolution could be divided into three stages. First, the relative cross-sectional area had no obvious changes. The coarsening of solder matrix even led to a slight decrease of resistance at this period. Second, the cross-sectional area reduction at peak and valley temperature was almost consistent and increased slowly because of the Joule heating. It was believed that Joule heating effect alleviated the crack nucleation and propagation by introducing the high current density to the solder. The low extreme temperature was improved by electric current and helped to retard the effect of thermal cycling. Third, the
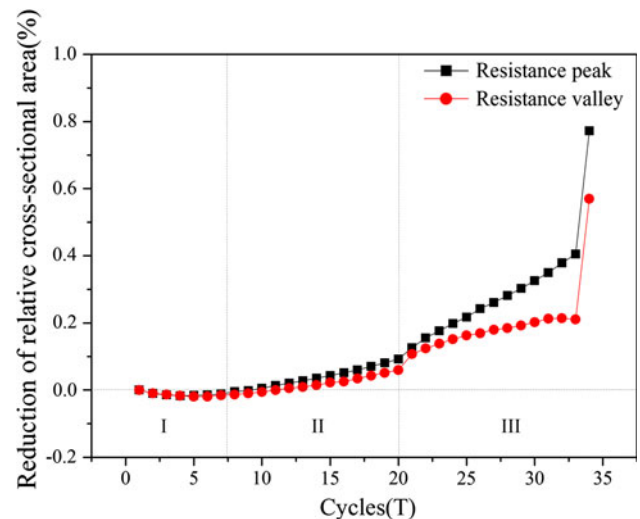
Fig. 10 Reduction of relative cross-sectional area with cycle numbers under the coupling effect of thermal cycling and EM
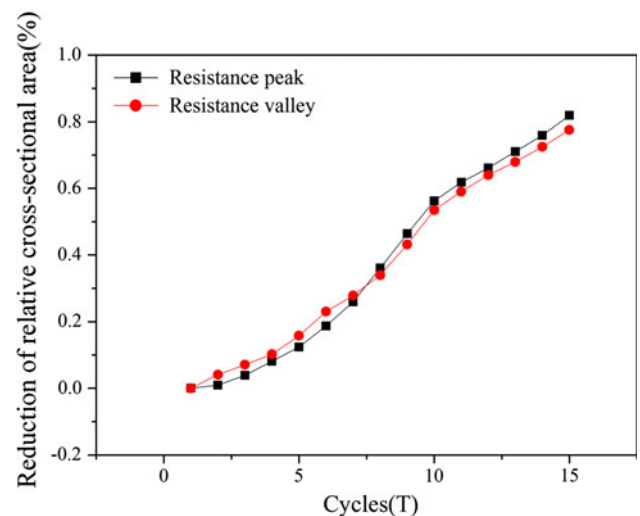
Fig. 11 Reduction of relative cross-sectional area with cycle numbers under the thermal cycling effect

cross-sectional area reduction became faster and caused the final failure of the joint as the evidence of the abrupt change caused by mass transportation. Although, the crack nucleation had been suppressed by Joule heating effect, crack continues growth. The contact area reduced subsequently and further enhanced the current density and accelerated EM damage. Metal atoms migrated from the cathode to the anode and trigger the growth of cracks at this side. The electric current became harmful at this stage and booted the broken joint by producing excessive Joule heating. Figure 11 shows the reduction of relative cross-sectional area with cycle numbers under the thermal cycling condition. It was demonstrated that the cross-sectional area of solder joint reduced continuously through the joint lifetime without EM effect.

Conclusions

The coupling effect of thermal cycling and EM on solder joint was investigated. The comparison tests with individual factors were also carried out. The conclusions were as follows:

1. The effect of cracks nucleation and propagation at low extreme temperature during thermal cycling process on the raise of resistance was far more severe than the phase segregation.
2. The resistance evolution under the coupling effect could be divided into three stages. First, resistance dropped slightly due to the phase coarsening. Second, Joule heating made the resistance increased slowly. Third, EM led to the rapid increase of the resistance and the final failure of the joint.
3. The application of high current density could help to improve the reliability of the solder joint under the coupling effect of thermal cycling and EM at the initial stage, but EM is harmful to the consequence process.

References

1. Plumbridge WJ (1996) J Mater Sci 31(10):2501. doi:10.1007/BF00687275
2. Lee JG, Subramanian KN (2003) J Electron Mater 32(6):523
3. Liu J, Salmela O, Sarkka J, Morris JE, Tegehall PE, Andersson C (2011) Reliability of microtechnology: interconnects, devices and systems. Springer, New York
4. Miao HW, Duh JG, Chiou BS (2000) J Mater Sci 11(8):609. doi:10.1023/A:1008928729212
5. Pang HLJ, Tan KH, Shi XQ, Wang ZP (2001) Mater Sci Eng A Struct 307(1–2):42
6. Pang JHL, Low TH, Xiong BS, Luhua X, Neo CC (2004) Thin Solid Films 462:370
7. Chen C, Tong HM, Tu KN (2010) Annu Rev Mater Res 40(1):531
8. Ma LM, Xu GC, Sun J, Guo F, Wang XT (2011) J Mater Sci 46(14):4896. doi:10.1007/s10853-011-5401-3
9. Lee A, Liu W, Ho CE, Subramanian KN (2007) J Appl Phys 102(5):053507
10. Ho CE, Lee A, Subramanian KN, Liu W (2007) Appl Phys Lett 91(2):021906
11. Chen C, Liang SW (2007) J Mater Sci 18(1–3):259. doi:10.1007/978-0-387-48433-4_17
12. Ma LM, Guo F, Xu GC, Wang XT, He HW, Zhao HY (2012) J Electron Mater 41(2):425
13. Zhou W, Liu L, Li B, Wu P (2010) Thin Solid Films 518(20):5875
14. He HW, Xu GC, Guo F (2010) J Mater Sci 45(4):929. doi:10.1007/s10853-009-4022-6
15. Liu HY, Zhu QS, Wang ZG, Shang JK (2011) Mater Sci Eng Struct 528(3):1467
16. Choi WJ, Yeh ECC, Tu KN (2003) J Appl Phys 94(9):5665
17. Cook B, Anderson I, Harringa J, Kang S (2003) J Electron Mater 32(12):1384
18. Sun J, Xu GC, Guo F (2011) J Mater Sci 46(10):3544. doi:10.1007/s10853-011-5265-6
19. He HW, Xu GC, Guo F (2010) J Mater Sci 45(2):334. doi:10.1007/s10853-009-3939-0
20. Agarwal R, Ou SE, Tu KN (2006) J Appl Phys 100(2):024909